



Determination of Some Petrophysical Properties of Reservoir Rocks in the Niger Delta

A. Akintola Sarah¹, U. Akpabio Julius^{1,2*} and C. Nduamaka Francis¹

¹Department of Petroleum Engineering, University of Ibadan, Ibadan, Nigeria.

²Department of Chemical and Petroleum Engineering, University of Uyo, Uyo, Nigeria.

Authors' contributions

This work was carried out in collaboration between all authors. Author AAS designed the study and wrote the protocol and author UAJ wrote the first draft of the manuscript and part of the literature searches. Author CNF managed the literature searches and the experimental process. All authors read and approved the final manuscript.

Article Information

DOI: 10.9734/JSRR/2015/15096

Editor(s):

(1) Shahid Naseem, Department of Geology, University of Karachi, Pakistan.

(2) Leszek Labedzki, Institute of Technology and Life Sciences, Kujawsko-Pomorski Research Centre, Poland.

Reviewers:

(1) Anonymous, Malaysia.

(2) Anonymous, Nigeria.

Complete Peer review History: <http://www.sciencedomain.org/review-history.php?iid=751&id=22&aid=7751>

Original Research Article

Received 5th November 2014
Accepted 17th December 2014
Published 10th January 2015

ABSTRACT

In formation evaluation, the knowledge of porosity, permeability and fluids saturation are very important in the determination of the hydrocarbon in place. These petro physical properties are necessary to understand the nature of the reservoir and help for proper field development planning. This was aimed at determining the petro physical properties (pore volume, bulk volume, grain volume, permeability and fluid saturation) of a reservoir from core plugs. A total of ten core plugs were used in this work. Archimedes immersion method was used in the determination of the bulk volume. Liquid saturation method was used in the determination of the porosity. The Dean-Stark extraction method was used in the determination of fluid saturation. From the results obtained in the core analysis, the sandstone reservoir has an average porosity of $14.9 \pm 5.1\%$, very good permeability with an average value of 349.77 ± 0.3 mD and a very large water saturation value of $82 \pm 0.4\%$. Consequently the hydrocarbon saturation is approximately 18%. This implies that the formation is not commercially viable to develop based on the hydrocarbon saturation. The study shows that experimental work is one of the valid tools for making informed decisions on the development of a field in the petroleum industry and highlights the importance of the basic petrophysical properties in reservoir management.

*Corresponding author: Email: juliakpabio@yahoo.com;

Keywords: Core analysis; fluid saturation; permeability; petrophysical properties; porosity; reservoir.

ABBREVIATIONS

A = Tortuosity factor; *A* = Cross-sectional Area; ANN = Artificial Neural Network; API = American Petroleum Institute; BV= Bulk Volume; EPT = Electromagnetic Propagation Tool; *F* = Formation Resistivity Factor; *GV* = Grain Volume; *K* = Permeability; *L* = Length; *LWD* = Logging While Drilling; *NMR* = Nuclear Magnetic Resonance; *P* = Pressure; *PNP* = Pulsed Neutron Porosity; *PV* = Pore Volume; *Q* = Flow rate; *R* = Resistivity; *RI* = Resistivity Index; *S* = Saturation; *T* = Temperature; μ = viscosity.

SUBSCRIPTS

g=gas; *h*=hydrocarbon; *o*= oil; *t*=true or total; *w*= Water.

SUPERSCRIPT

n= saturation exponent; *m*= cementation factor.

1. INTRODUCTION

One of the most important tasks in reservoir engineering is characterizing different parameters of the reservoir. Water saturation is a parameter which helps in evaluating the volume of hydrocarbon in reservoirs. Determination of this parameter started from 1942 by integrating some well logs in clean sandstones [1]. When the water saturation is determined then the hydrocarbon saturation can be calculated from Equation (1):

$$S_h = 1 - S_w \tag{1}$$

Where: S_h is the hydrocarbon saturation and S_w is the water saturation.

Archie introduced an equation, which relates resistivity index (RI) and formation resistivity factor (*F*) in order to calculate water saturation. Using this equation, water saturation is computed although it cannot be applied to the shaly section of the reservoir [1]. The final outcome of Archie’s work was an equation for the calculation of water saturation based on certain parameters given in Equations (2) and (3).

$$S_w = \left(\frac{1}{RI} \right)^{\frac{1}{2}} = \left(\frac{F * R_w}{R_t} \right)^{\frac{1}{2}} \tag{2}$$

$$S_w^n = \frac{a R_w}{\phi^m R_t} \tag{3}$$

Where $F = \frac{R_o}{R_w}$ (4)

and

$$RI = \frac{R_t}{R_o} \tag{5}$$

And S_w = Water saturation, *RI* = Resistivity index, *F* = Formation Resistivity Factor, R_w = water Resistivity, R_t = Total or true Resistivity for both formation water and hydrocarbon, R_o = Resistivity of 100% brine *n* = saturation exponent, *a* = Tortuosity factor ϕ = Porosity and *m* = cementation factor.

An electromagnetic propagation tool (EPT) of Schlumberger was used to measure water saturation in the invaded zone without the need for other resistivity logs or Archie’s equation. The EPT was useful in determining both hydrocarbon saturation and fluid mobility in fields with variable or freshwater resistivities, with vugular porosity or with oil-based muds [2].

A new application, which has been proven to be very useful to supplement conventional saturation evaluations, is the diffusion NMR (Nuclear Magnetic Resonance) method. This is applied on fluids contained in porous rocks to interpret oil saturation quantitatively. This method utilizes the differences in molecular self-diffusion between oil and water. It has been applied successfully to data recorded in wells that contain heavy oil. The NMR-derived saturations are in good agreement with core and log data as verified by Looyestijn [3].

Balch et al. [4] predicted the water saturation in a sandstone reservoir in Mexico using artificial intelligence and seismic attributes. Three dimensional seismic data and values of water saturation at 19 wells were used; the first step was a fuzzy logic algorithm to detect five attributes (reflection coefficient, frequency, instantaneous phase, amplitude and energy) that were strongly correlated with water saturation. Then, a back propagating Artificial Neural Network (ANN) was used to find the relationship between these attributes and the value of water saturation. The main contribution in the study by them was the use of seismic attributes for water saturation estimation [4].

Boadu [5] studied the effect of change in oil saturation level on seismic wave velocities and their ratio in a laboratory experiment. He applied changes to the temperature and values of oil saturation and used an ANN to observe a relationship between these variables and the values of P and S wave velocities and their ratios.

Parameters in Archie's equation are usually determined through experiments on the electric properties of rocks. Saturation should be measured in well-preserved cores since large errors may exist between the measured values and the original values due to degasification and volatilization [6].

One of the most interesting studies in this field was the work of Mu and Cao with a physical model of a sandstone reservoir [7]. They isolated the model and drilled two holes, injecting and discharging into them. Saturating the sandstone layer with water, oil, CO₂ and CH₄ from 10 to 100 percent respectively, they succeeded in simulating seismic surveying by application of ultrasonic data acquisition; thereby, creating an environment to study the effect of change in the fluids type and saturation value on P-wave amplitude and absorption coefficient. The outcome of their study was an expression for determining absorption coefficient profile using Biot theory and reflection amplitude spectrum. More recently, interpreters have used seismic attributes to evaluate water saturation values directly or estimating proper rock physical properties such as shale volume which are useful in water saturation estimation process [8].

For reservoir evaluation purposes, two basic approaches may be used to determine porosity: cores may be cut and analyzed, with the porosity

values determined by direct measurement and porosity values may be calculated from the log data obtained through downhole wireline tools; Jenkins [9] used the first approach in his work.

Pulsed Neutron Porosity (PNP) logging is a new method of determining formation porosity in which the die-away of epithermal neutrons with time is measured following emission of pulses of neutrons. The pulsed neutron technique offers superior porosity sensitivity and decreased lithology dependence in comparison to steady-state neutron porosity logs [10]. In the work of determination of porosity in horizontal wells, it was found that LWD (Logging While Drilling) maximum density derived porosity provides the best estimate of the true formation porosity in the horizontal well studied [11].

A detailed study of a number of methods for measuring relative permeability has been made in a search for the technique most suitable for routine analysis of cores taken from reservoir rocks. To determine relative permeability-saturation relations of samples of reservoir rock in the laboratory, it is important to know the factors that affect these measurements; to ascertain their magnitude and then take steps to eliminate or minimize them. These factors include the boundary effect, the gas expansion effect and the rate effect [12].

Measurement of the relative permeability of gas condensate is typically done through steady state linear core flood experiments using model fluids. App and Burger [13] performed three pseudo-steady state linear core flood experiments to estimate the effective gas and condensate relative permeabilities for a rich gas condensate system using live single phase reservoir fluid. Relative permeability is an important petrophysical parameter needed for characterization of multiphase flow in petroleum reservoirs. From a two-phase flow in a porous media, relative permeability data can be determined by interpretation of laboratory displacement tests on cylindrical core plugs [14]. The objective of the research therefore is to determine the Petrophysical properties of reservoir rocks to ascertain that there is hydrocarbon in commercial quantity to justify further development of the field.

1.1 Petroleum Geology of the Niger Delta

The Niger Delta province is a geologic province in the Niger Delta area of Nigeria in West Africa

also called the Niger Delta Basin see Fig. 1. This area contains one petroleum system called the "Tertiary Niger delta (Akata-Agbada) Petroleum System". Most part of it lies within the borders of Nigeria and is bounded by the Gulf of Guinea which is part of the eastern tropical Atlantic Ocean off the western African coast. The area contains as much as 34.5 billion barrels ($5.5 \times 10^9 \text{ m}^3$) of recoverable oil and 94 trillion cubic feet ($2.7 \times 10^9 \text{ m}^3$) of natural gas at the origin. This field contains thousands of individual reservoirs, most of which are sandstone pockets trapped within oil-rich shale strata. The Niger Delta region has as many as 574 fields discovered (481 oil and 93 natural gas fields). The Success rate of hitting oil in the past has been as high as 45% [16]. The core samples collected for this research was in this area in Port Harcourt – the eastern part of the region.

The delta proper began developing in the Eocene, accumulating sediments which are now over 10 kilometers thick. The upper Akata Formation (the marine-shale facies) is the primary source rock of the delta, and contribution from the lowermost Agbada Formation which is the interbedded marine shale. Petroleum is produced from sandstone facies within the Agbada Formation, however, turbidite sand in the upper Akata Formation is a potential target in deep water offshore and possibly beneath currently producing intervals onshore [17].

The delta area is divided into three gross lithofacies: (i) marine claystones and shales of unknown thickness, at the base; (ii) alternations of sandstones, siltstones and claystones, in which the sand percentage increases upwards and (iii) alluvial sands, at the top [18].

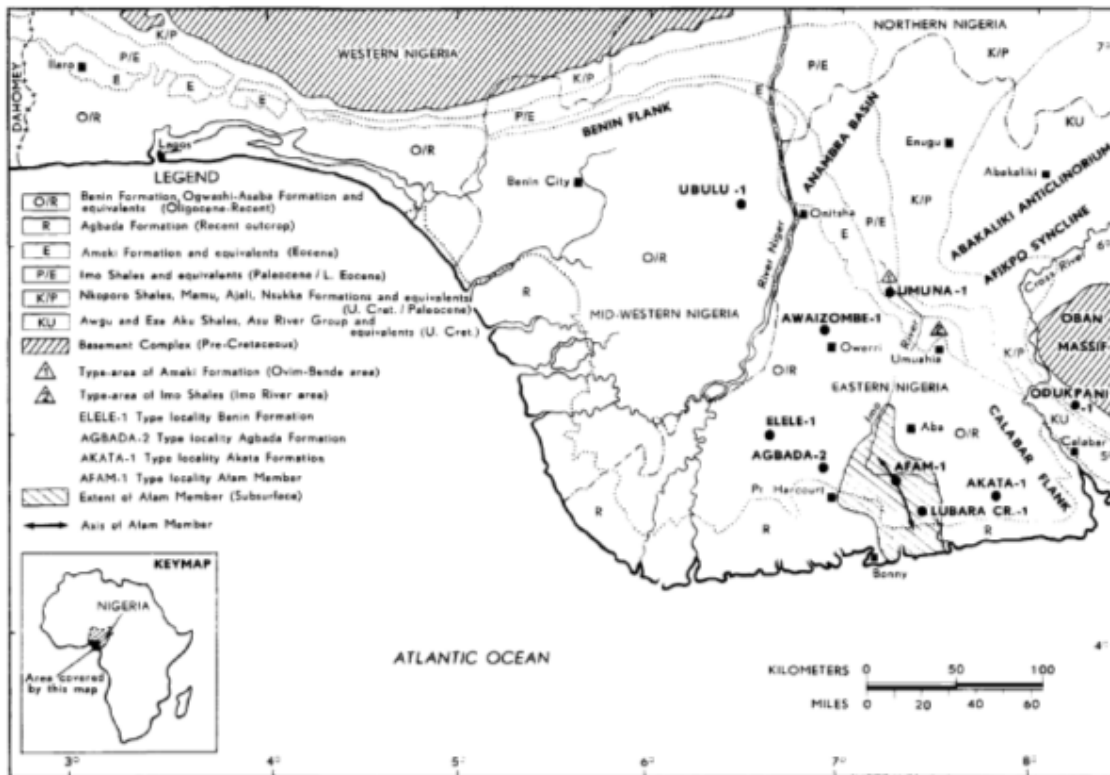


Fig. 1. Map of southern part of Nigeria showing the Niger delta and outcrops of Cretaceous and tertiary formations [15]

2. MATERIALS AND METHODS

Ten core samples were obtained at different depths in a formation and used for the study.

2.1 Bulk volume Determination

Bulk volume of a core plug can be determined by several methods and Archimedes immersion method was used applied in this work. The apparatus required include an analytical balance accurate to one milligram, fine wire cradle, liquid container, thermometer and a pressure saturator. The sample is saturated with brine of known density; excess liquid is carefully removed from sample, avoiding grain loss. A beaker is filled with the saturating liquid and placed in a balance and a fine wire cradle is lowered into the liquid to a reference mark. The saturated sample is then placed on the cradle, submerged to the reference mark and the immersed weight of the sample is obtained. The bulk volume was calculated using Equation (6) and the results is presented in Table 1.

$$BV = \frac{\text{Immersed weight}}{\text{Densit of immersion Fluid}} \quad (6)$$

2.2 Determination of Effective Porosity

The liquid saturation method was used in the determination of effective porosity. Weight of a dry, clean sample which has been desiccated is obtained and saturated with brine water for four hours. The sample is removed from the saturating vessel and weighed submerged in the saturating liquid; finally excess liquid is carefully removed and the saturated sample is weighed in air. The following equations are used to calculate the porosity:

$$PV = \frac{\text{Saturated Weight} - \text{Dry Weight}}{\text{Saturated Weight} - \text{Im mersed Weight}} \quad (7)$$

$$\text{Porosity} = \frac{BV - GV}{BV} \quad (8)$$

Where PV = Pore Volume, BV = Bulk Volume and GV = Grain Volume.

The results of the experiment are shown in Table 2.

2.3 Permeability Determination

The apparatus for the experiment are a gas permeameter, core holder, nitrogen gas and stopwatch. The sample is placed in a core holder and connected to the permeameter and nitrogen in passed through it by laminar flow. The flow rate is measured with a bubble tube and record the upstream pressure from the gauge of the regulator. The permeability is calculated using the Equation (9)

$$K = \frac{\mu QL}{A\Delta P} \quad (9)$$

Where, K = permeability, μ = viscosity of nitrogen gas, Q= flow rate, L= length of core sample, A= cross sectional area of the sample and ΔP = upstream pressure-downstream pressure. Table B-1 in the Appendix shows the spreadsheet of permeability calculation.

2.4 Fluid Saturation Determination

The Dean-Stark extraction method was used in the determination of saturation of the core plugs. The following apparatus are used: Dean-Stark apparatus, Toluene, weighing balance, Oven and Thimbles.

The distillation extraction (Dean-Stark) method of determining fluid saturation depends upon the distillation of the water fraction, and the solvent extraction of the oil fraction from the sample. The sample is weighed and the water fraction is vaporized by boiling solvent. The water is condensed and collected in a calibrated receiver. Vaporized solvent also condenses, soaks the sample and extracts the oil. The sample is oven-dried, weighed and finally the oil content is determined by gravimetric difference.

The following calculations were used:

$$\text{Weight\% Water (Gravimetric)} = \frac{\text{Weight of Water} * 100}{(\text{Initial Sample Weight})} \quad (10)$$

or

$$\text{Weight\% Water (Volumetric)} = \frac{(\text{Volume of Water}) * (\text{Density of Water}) * 100}{(\text{Initial Sample Weight})} \quad (11)$$

$$\text{Weight of Solids (Gravimetric)} = \frac{\text{Dry Weight of Sample} * 100}{(\text{Initial Sample Weight})} \quad (12)$$

$$\text{Weight of Oil (Gravimetric)} = \frac{(\text{Initial Weight} - \text{Dry Weight} - \text{Weight of Water}) * 100}{(\text{Initial Sample Weight})} \quad (13)$$

The saturations are normally expressed as percentages of the sample pore space and this requires the sample porosity, water density and oil density for the calculations. Therefore, the water and oil saturations are obtained with the formula:

$$\% \text{ Water} = \frac{\text{Volume of Water} * 100}{(\text{Pore Volume})} \quad (14)$$

and

$$\% \text{ Oil} = \frac{(\text{Weight of Oil}) / (\text{Density of oil}) * 100}{(\text{Pore Volume})} \quad (15)$$

Table 1. Bulk Volumes of the core plugs

| Sample # | Bulk volume(cc) | Dry weight(g) | Wet weight(g) | Immersed weight(g) |
|----------|-----------------|---------------|---------------|--------------------|
| 596 | 62.93 | 147.79 | 150.1 | 87.17 |
| 612 | 54.86 | 126.02 | 129.87 | 75.01 |
| 595 | 74.9 | 149.06 | 162.29 | 87.39 |
| 597 | 63.01 | 129.24 | 139.75 | 76.74 |
| 602 | 67.52 | 138.27 | 149.55 | 82.03 |
| 603 | 58.04 | 115.08 | 124.96 | 66.92 |
| 610 | 62.26 | 123.16 | 133.51 | 71.25 |
| 611 | 52.93 | 106.53 | 115.84 | 62.91 |
| 626 | 56.03 | 119.67 | 130.04 | 74.01 |
| 635 | 68.73 | 138.61 | 150.34 | 81.61 |

Table 2. Bulk volume and porosities at different depths of core plugs

| Sample # | Depth (m) | Dry wt.(g) | Wet wt.(g) | immersed wt.(g) | Grain vol.(g) | Grain dens(g/cc) | Pore vol.cc) | Bulk vol.(cc) | Porosity (%) |
|----------|-----------|------------|------------|-----------------|---------------|------------------|--------------|---------------|--------------|
| 596 | 3370 | 147.79 | 150.1 | 87.17 | 60.62 | 2.44 | 2.31 | 62.93 | 3.7 |
| 612 | 3371 | 126.02 | 129.87 | 75.01 | 51.01 | 2.47 | 3.85 | 54.86 | 7.0 |
| 595 | 3372 | 149.06 | 162.29 | 87.39 | 61.67 | 2.42 | 13.23 | 74.9 | 17.7 |
| 597 | 3373 | 129.24 | 139.75 | 76.74 | 52.5 | 2.46 | 10.51 | 63.01 | 16.7 |
| 602 | 3374 | 138.27 | 149.55 | 82.03 | 56.24 | 2.46 | 11.28 | 67.52 | 16.7 |
| 603 | 3375 | 115.08 | 124.96 | 66.92 | 48.16 | 2.39 | 9.88 | 58.04 | 17.0 |
| 610 | 3376 | 123.16 | 133.51 | 71.25 | 51.91 | 2.37 | 10.35 | 62.26 | 16.6 |
| 611 | 3377 | 106.53 | 115.84 | 62.91 | 43.62 | 2.44 | 9.31 | 52.93 | 17.6 |
| 626 | 3378 | 119.67 | 130.04 | 74.01 | 45.66 | 2.62 | 10.37 | 56.03 | 18.5 |
| 635 | 3379 | 138.61 | 150.34 | 81.61 | 57 | 2.43 | 11.73 | 68.73 | 17.1 |

$$\% \text{ Gas} = 100 - \% \text{ Water} - \% \text{ Oil} \quad (16)$$

The Equations (10) to (16) have been used to calculate the values of the fluid saturations as shown in Table 3.

3. RESULTS AND DISCUSSION

The routine core analysis measurements were provided in excel spreadsheet format and the measurements were available for horizontal plugs which includes; grain density, porosity, air permeability, and fluid saturations. Core photos were available and are presented in Appendix A in Fig. A-1. and the experimental set up in Figs. A-2 and A-3. Appendix B contains the results in excel spreadsheet Table B-1. and the conventional results of the core experiment are shown in Table B-2.

Table 4 is the summary of the result of the study showing the values of porosity, permeability and fluid saturations. The average value of the porosity was $14.86 \pm 5.10\%$; average permeability was $349.77 \pm 242.98 \text{ mD}$; average water saturation was $81.93 \pm 5.56\%$; average oil saturation was $4.38 \pm 3.15\%$ and the average gas saturation was $13.69 \pm 5.07\%$

3.1 Interpretation of Core Porosity

After cleaning of the core plugs and removal of fluids, porosity is determined from the grain volume and the bulk volume of the sample. Depending on the technique used, different types of porosity are estimated. Porosity measurement by the liquid saturation method indicates only pores that are interconnected (effective porosity) thereby providing a very good estimate of effective porosity for the purpose of reservoir evaluation.

The porosities of petroleum reservoirs range from about 5% to 45% and factors determining

the magnitude of porosity in sediments are grain sorting, degree of cementation or consolidation, amount of compaction and methods of grain packing [18]. If all the grains are of the same size, sorting is said to be good and porosity may be high. If grains are of many sizes and are mixed together, sorting is regarded as poor and porosity in that condition will be reduced. Cementation that takes place during diagenesis also tends to fill in the pore space, so highly cemented sedimentary rocks have lower porosity than poorly cemented sedimentary rocks. Although, round grains and a high content of grain cement gives a high porosity, and angular grains and low cement content yields lower porosity.

The core porosity values of core plugs ranges from 3.7% to 17.1% at the cored interval. The low porosity values were observed in intervals that are associated with claystones and siltstone interbedded lamina. The relatively high porosity interval was observed in massive sandstones intervals that are very fine to fine grains and are well sorted as observed in depth of 3379 to 3372 m (Fig. 2).

The low porosity intervals were 3370 and 3371 m which are likely laminated shaly intervals. The average porosity was 14.86, with a standard deviation and variance of 5.10 and 26.06 respectively.

3.2 Interpretation of Permeability

The permeability of a rock is controlled by rock grain size, grain shape, degree of cementation or consolidation, grain packing, and clay. The value may vary from less than 1 mD to over 2000 mD. In the Niger Delta the value could be above 2000 mD in very permeable formations. The quality of a reservoir as determined by permeability in mD may be scaled as shown in the Table 5.

Table 3. Fluid Saturations of the Core Plugs

| Sample number | Wt. before dean stark(g) | Weight after dean stark(g) | Water produced(cc) | Oil weight(g) | Oil (%) | Water (%) | Gas (%) |
|---------------|--------------------------|----------------------------|--------------------|---------------|---------|-----------|---------|
| 596 | 149.78 | 147.79 | 1.90 | 0.092 | 4.7 | 82.2 | 13.1 |
| 612 | 129.43 | 126.02 | 3.38 | 0.033 | 1.0 | 87.7 | 11.3 |
| 595 | 161.84 | 149.06 | 12.08 | 0.697 | 6.2 | 91.3 | 2.5 |
| 597 | 138.27 | 129.24 | 8.70 | 0.331 | 3.7 | 82.8 | 13.5 |
| 602 | 148.12 | 138.27 | 9.77 | 0.077 | 0.8 | 86.6 | 12.6 |
| 603 | 122.95 | 115.08 | 7.36 | 0.512 | 6.1 | 74.5 | 19.4 |
| 610 | 131.74 | 123.16 | 7.96 | 0.625 | 7.1 | 76.9 | 16.0 |
| 611 | 114.57 | 106.53 | 7.21 | 0.831 | 10.5 | 77.4 | 12.1 |
| 626 | 128.44 | 119.67 | 8.66 | 0.115 | 1.3 | 83.5 | 15.2 |
| 635 | 147.81 | 138.61 | 8.96 | 0.239 | 2.4 | 76.4 | 21.2 |

Table 4. Result of porosity, permeability and fluid saturation

| S/no | Depth(m) | porosity(%) | Perm. K(md) | Oil Saturation (%) | Water (%) | Gas (%) |
|------|----------|-------------|-------------|--------------------|-----------|---------|
| 596 | 3370 | 3.7 | 175.424 | 4.7 | 82.2 | 13.1 |
| 612 | 3371 | 7.0 | 244.222 | 1 | 87.7 | 11.3 |
| 595 | 3372 | 17.7 | 392.85 | 6.2 | 91.3 | 2.5 |
| 597 | 3373 | 16.7 | 904.124 | 3.7 | 82.8 | 13.5 |
| 602 | 3374 | 16.7 | 662.601 | 0.8 | 86.6 | 12.6 |
| 603 | 3375 | 17.0 | 182.942 | 6.1 | 74.5 | 19.4 |
| 610 | 3376 | 16.6 | 228.439 | 7.1 | 76.9 | 16 |
| 611 | 3377 | 17.6 | 228.347 | 10.5 | 77.4 | 12.1 |
| 626 | 3378 | 18.5 | 263.157 | 1.3 | 83.5 | 15.2 |
| 635 | 3379 | 17.1 | 215.642 | 2.4 | 76.4 | 21.2 |

Table 5. Permeability classification scale [19]

| Permeability values(mD) | Classification |
|--------------------------|----------------|
| Less than 1 | Poor |
| Between 1 and 10 | Fair |
| Between 10 and 50 | Moderate |
| Between 50 and 250 | Good |
| Above 250 | Very good |

670 mD) were indicated in depth interval of 3372 m to 3374 m. This may be attributed to the very fine to fine grain sandstone interval that is well-sorted. The depth 3370 m to 3371 also has good permeability values as the first depth interval (see Table 5 for permeability classifications).

3.3 Interpretation of Fluid Saturation

The summation of all saturations in a given rock must equal 100% and water saturation of a formation can vary from 100% to much smaller percentage but will never be zero because there is always a small amount of capillary water or irreducible water that cannot be displaced. Also for an oil or gas bearing reservoir rock, all the hydrocarbon saturation cannot be removed or displaced, some of the oil or gases remain trapped in the pore volume and this hydrocarbon saturation is regarded as residual or irreducible oil saturation.

The permeabilities of core plugs were measured horizontally. The horizontally measured permeability is accepted as the rock permeability because it is measured parallel to the bedding which is the major contributor to fluid flow into a typical reservoir. Plot of permeability against depth in linear scale is given in Fig. 3.

Good permeability values seen in the depth interval of 3379 m to 3375 m in the plot is because of the clay stones lamination interval which acts as a barrier to the permeability. Very good permeability values (390 mD, 900 mD and

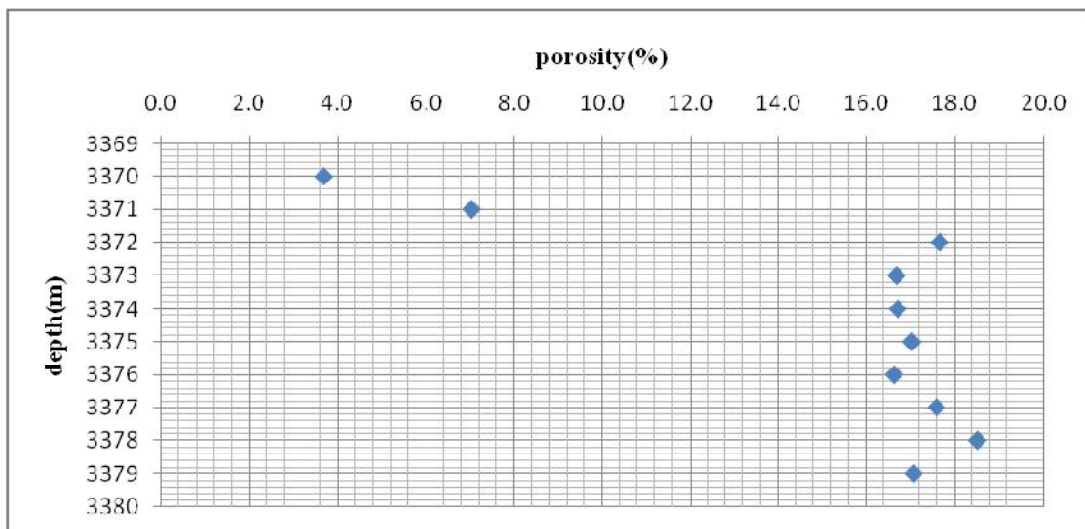


Fig. 2. Core porosity versus depth

Three types of fluid saturation values, water, gas and oil were reported in the sampled well. The average water saturation (S_w) was 81.93%; average gas saturation (S_g) was 13.69% and average oil saturation (S_o) was 4.38%. Fig. 4 shows the plot of fluid saturation versus depth of the core samples.

at depth 3375 m to 3377 m but the value is too small to require the development of the formation. From the result of the fluid saturation, it can be seen that the rock is basically a water-bearing rock with little quantity of hydrocarbons. This type of formation cannot be exploited because is the size of the hydrocarbon.

The plot of fluid saturation versus depth presents an interval of increasing hydrocarbon saturation

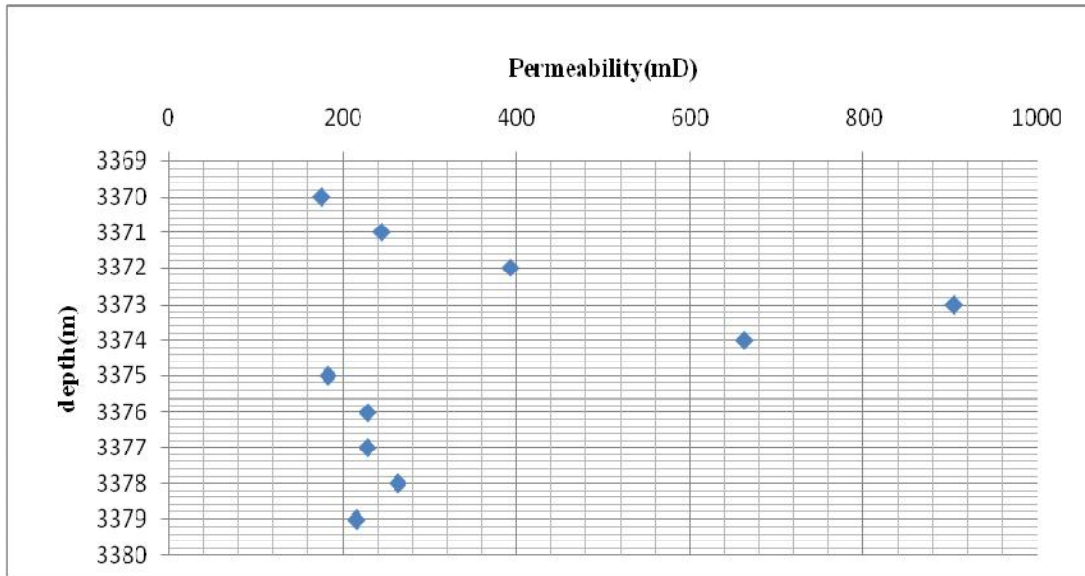


Fig. 3. Permeability versus depth plot

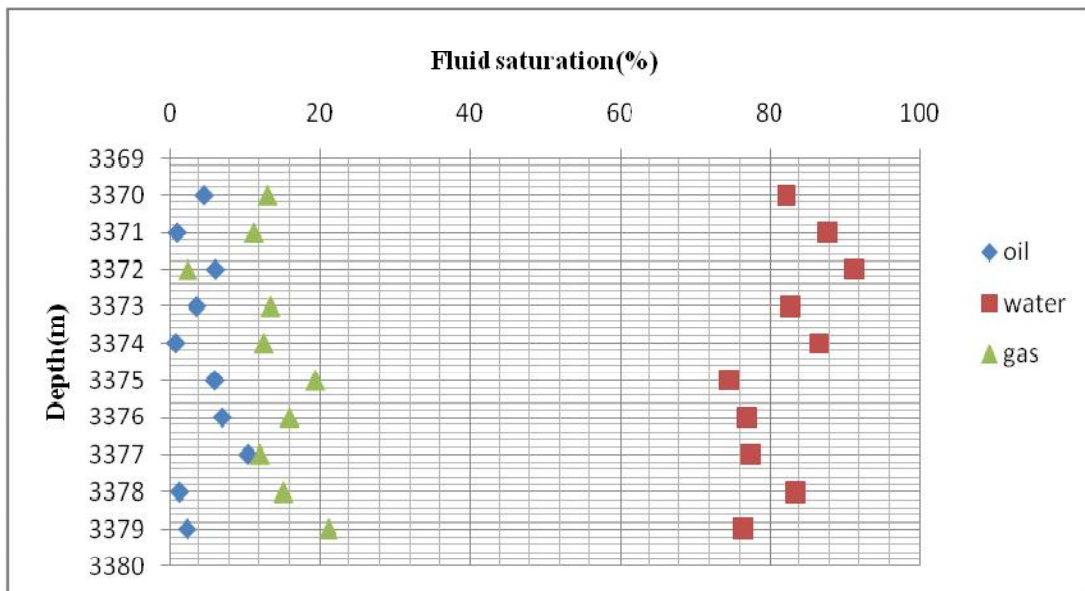


Fig. 4. Fluid saturation versus depth

4. CONCLUSION

From the laboratory experiments, the following conclusions can be made:

- i. Water saturation, porosity and permeability of ten core samples were determined and the results show that the reservoir rocks do not contain hydrocarbon in commercial quantity and therefore should not be developed.
- ii. The value of the average porosity was 15% which is good; the average permeability was 350 mD which is also very good. However, the water saturation was 82% which implies that the hydrocarbon saturation is 18% showing that the formation is a water-bearing rock and cannot be drilled for hydrocarbon.
- iii. This experiment can help the petroleum engineer to make informed and accurate decision on reservoir management, primarily based on fluid saturation information.
- iv. It is recommended that other methods should be used to determine these petrophysical properties to confirm the results of these single methods.
- v. Artificial Neural Network method may be used in future studies to predict permeability, porosity and water saturation of the reservoir core samples and confirm results of this study.
- vi. Integration should be made of the different approaches used in the determination of water saturation whereby results obtained from the use of well logs, core data and seismic attributes are correlated to obtain far more robust results.

COMPETING INTERESTS

Authors have declared that no competing interests exist.

REFERENCES

1. Archie GE. The electrical resistivity log as an aid in determining some reservoir characteristics, trans. AIME. 1942;54(62):146.
2. Gilmore RJ, Clark B, Best D. Enhanced saturation determination using the EPT-G end fire antenna array SPWLA 28th Annual logging symposium London. England; 1987.
3. Looyestijn WJ. Determination of Oil Saturation from diffusion NMR logs SPWLA 37th Annual logging symposium; 1996.
4. Balch RS, Stubbs BS, Weiss WW, Wo S. Using artificial intelligence to correlate multiple attributes to reservoir properties, SPE, 56733 prepared for presentation at the SPE. Annual Technical Conference and Exhibition held in Houston Texas; 1999
5. Boadu FK. Predicting oil saturation from velocities using petrophysical models and artificial neural networks, J. Petroleum Sci. Eng. 2001;30:143-154.
6. Chen X. Kuang, LC, Sun ZC. Archie parameter determination by analysis of saturation data research note on petrophysics. 2002;43(2):103-107.
7. Mu YG, Cao SY. Seismic physical modeling and sandstone reservoir detection using absorption coefficients of seismic reflections. J. Petroleum Sci. Eng. 2004;41:159-167.
8. Alimoradi A, Moradzadeh A, Bakhtiari MR. Methods of water saturation estimation: historical perspective. Journal of Petroleum and Gas Engineering 2011;2(3):45-53.
9. Jenkins RJ. Accuracy of porosity determinations SPMLA first annual logging symposium, Tulsa, Oklahoma; 1960.
10. Mills WR, Stromswold, DC, Allen LS. Pulsed neutron porosity logging SPWLA 29th Annual logging symposium; 1988.
11. Calvert S, Lovell M, Harvey P, Samworth JR, Hook J. Porosity determination in horizontal wells SPWLA 39th Annual logging symposium, keystone, Colorado; 1998.
12. Richardson JG, Kerver JK, Hafford JA. Osoba JS. Laboratory determination of relative permeability society of petroleum engineers trans. AIME. 1953;195.
13. App JF, Burger JE. Experimental determination of relative permeability of a rich gas condensate system using live fluid SPE 109810 prepared for presentation at the SPE. Annual Technical Conference and Exhibition held in Anaheim L California, USA; 2007.
14. Ubani CE, Ikisimama SS, Onyekonwu MO. Experimental determination of relative permeability from unconsolidated core samples of the Niger delta SPE 172478 prepared for presentation at the Nigeria

- .Annual International Conference and Exhibition held in Lagos Nigeria; 2014.
15. Short KC. Stauble AJ. Outline of Geology of Niger delta. The American Association of Petroleum Geologists Bulletin. 1967;5(5):761-779.
 16. The Niger delta Province; 2014.
Available:http://en.wikipedia.org/wiki/Niger_Delta_province
 17. Tuttle MW, Charpentier RR. Brownfield ME. The Niger delta petroleum system: Niger delta Province, Nigeria, Cameroon, and Equatorial Guinea, Africa. U.S. geological survey open file report 99-50H; 1999.
 18. Doust H. Reconstruction of the evolution of the Niger River and implications for sediment supply to the Equatorial Atlantic margin of Africa during the Cretaceous and the Cenozoic Geological Society, London. Special Publications. 2014;386:327-349. DOI:10.1144/SP386.20.
 19. Djebbar T, Donaldson EC. Petrophysics Third Edition: Theory and practice of measuring reservoir rock and fluid transport properties. Gulf Professional Publishing; 2011.

APPENDICES

APPENDIX A



Fig. A-1. Core plugs for the study



Fig. A-2. Setup of the nitrogen gas permeameter to determine plugs' permeability

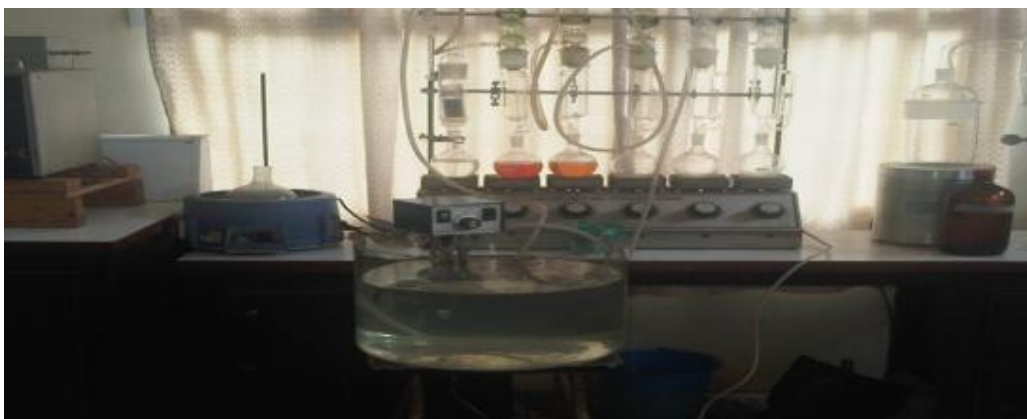


Fig. A-3. Setup of the dean-stark apparatus

APPENDIX B

Table B-1. Excel worksheet showing the template used in calculating permeability of the plugs Insert Table B-1.

Table B-1. Calculation of core sample permeability

| Sample number | Test Press. (psi) | Baro. Pressure (inches) | Temp (°C) | Gas Viscosity (cP) | Volume Timed (cc) | Ave Time (secs) | Length (cm) | Diameter (cm) | Pressure (P) (atm) | Flow rate (Q) (cc/sec) | Area (A) (Cm²) | Barometric (B) (atm) | Permeability (K) (mD) |
|----------------------|--------------------------|--------------------------------|------------------|---------------------------|--------------------------|------------------------|--------------------|----------------------|---------------------------|-------------------------------|----------------------------------|-----------------------------|------------------------------|
| 595 | 0.5 | 30.61 | 25 | 0.017747 | 25 | 20.5 | 6.944 | 3.736 | 0.032798 | 1.186585 | 11.17016 | 1.023027 | 392.9 |
| 596 | 0.2 | 30.6 | 25.2 | 0.017756 | 25 | 128.82 | 6.995 | 3.747 | 0.012384 | 0.194069 | 11.02843 | 1.022693 | 175.4 |
| 597 | 0.2 | 30.65 | 25 | 0.017747 | 25 | 19.69 | 5.797 | 3.79 | 0.012384 | 1.235399 | 11.283 | 1.024364 | 904.1 |
| 602 | 0.2 | 30.67 | 26 | 0.017792 | 25 | 28.56 | 6.082 | 3.77 | 0.012384 | 0.851716 | 11.16423 | 1.025033 | 662.6 |
| 603 | 0.2 | 30.65 | 25 | 0.017747 | 25 | 88.22 | 5.225 | 3.779 | 0.012384 | 0.275731 | 11.2176 | 1.024364 | 182.9 |
| 610 | 0.2 | 30.6 | 25 | 0.017747 | 25 | 72.47 | 5.468 | 3.817 | 0.012384 | 0.335656 | 11.44433 | 1.022693 | 228.4 |
| 611 | 0.2 | 30.62 | 25 | 0.017747 | 25 | 69.72 | 5.016 | 3.728 | 0.012384 | 0.348896 | 10.91687 | 1.023362 | 228.3 |
| 612 | 0.2 | 30.65 | 25 | 0.017747 | 25 | 75.2 | 5.883 | 3.759 | 0.012384 | 0.323471 | 11.09918 | 1.024364 | 244.2 |
| 626 | 0.2 | 30.65 | 25 | 0.017747 | 25 | 68.47 | 5.677 | 3.728 | 0.012384 | 0.355265 | 10.91687 | 1.024364 | 263.2 |
| 635 | 0.2 | 30.6 | 25 | 0.017747 | 25 | 90.3 | 6.351 | 3.793 | 0.012384 | 0.26938 | 11.30087 | 1.022693 | 215.6 |

Table B-2. Result of conventional core measurement of the core plugs

| S/no | Bulk vol(cc) | Dry wt(g) | Wet wt(g) | Immersed wt(g) | Grain vol(g) | Grain density (g/cc) | Pore vol(cc) |
|------|--------------|-----------|-----------|----------------|--------------|----------------------|--------------|
| 596 | 62.93 | 147.79 | 150.1 | 87.17 | 60.62 | 2.44 | 2.31 |
| 612 | 54.86 | 126.02 | 129.87 | 75.01 | 51.01 | 2.47 | 3.85 |
| 595 | 74.9 | 149.06 | 162.29 | 87.39 | 61.67 | 2.42 | 13.23 |
| 597 | 63.01 | 129.24 | 139.75 | 76.74 | 52.5 | 2.46 | 10.51 |
| 602 | 67.52 | 138.27 | 149.55 | 82.03 | 56.24 | 2.46 | 11.28 |
| 603 | 58.04 | 115.08 | 124.96 | 66.92 | 48.16 | 2.39 | 9.88 |
| 610 | 62.26 | 123.16 | 133.51 | 71.25 | 51.91 | 2.37 | 10.35 |
| 611 | 52.93 | 106.53 | 115.84 | 62.91 | 43.62 | 2.44 | 9.31 |
| 626 | 56.03 | 119.67 | 130.04 | 74.01 | 45.66 | 2.62 | 10.37 |
| 635 | 68.73 | 138.61 | 150.34 | 81.61 | 57 | 2.43 | 11.73 |

© 2015 Sarah et al.; This is an Open Access article distributed under the terms of the Creative Commons Attribution License (<http://creativecommons.org/licenses/by/4.0>), which permits unrestricted use, distribution, and reproduction in any medium, provided the original work is properly cited.

Peer-review history:

The peer review history for this paper can be accessed here:
<http://www.sciencedomain.org/review-history.php?iid=751&id=22&aid=7751>